Journal of Theoretical and Applied Vibration and Acoustics 4 (1) 19-36 (2018)

I S A V

Journal of Theoretical and Applied Vibration and Acoustics

journal homepage: http://tava.isav.ir

Analyzing dynamical snap-through of a size dependent nonlinear micro-resonator via a semi-analytic method

Soroush Sepehri[a], Hossein Mohammadi[a*]

[a] *School of Mechanical Engineering, Shiraz University, Shiraz, Islamic Republic of Iran*

ARTICLE INFO

Article history:
Received 15 February 2018

Received in revised form
28 May 2018

Accepted 9 June 2018

Available online 25 June 2018

Keywords:
MEMS

Bifurcation

Modified Strain Gradient

Stability

Nonlinear Vibration

ABSTRACT

In the present paper, the dynamical snap-through of a preloaded micro-sensor is analyzed. This behavior is linked to analyzing bifurcation behavior of the micro structure in a suitable framework. Effects of the axial pre-stress and the excitation amplitude on the stability and sensitivity of the sensor are also discussed. In order to capture the size effects, the modified strain gradient theory is employed on an Euler-Bernoulli beam. Applying the Hamilton's principle and utilizing the Galerkin's method, the nonlinear governing equation for the vibration is obtained. The method of multiple scales (MMS) is then used to obtain the frequency-response equation and by using a mathematical approach, the bifurcation points and the jump heights of the micro-resonator are analyzed. The calculated analytic equation for frequency response, provides the conditions for obtaining the range of snap-through and studying the effects of different designing parameters on the multivaluedness range. The jump height of the micro-resonator is proposed to use as a criterion for sensing purposes. The simulations are illustrated and the results are verified with similar works.

1. Introduction

Unique properties and characteristics have made Micro-electro-mechanical systems (MEMS) suitable for devices such as micro-resonators [1], micro-actuators [2], bio-MEMS [3] and so on. The usage of beam structures in MEMS has also been gaining widespread popularity among scholars. One such micro-electromechanical device in which beam structures have been

* Corresponding author:
E-mail address: h_mohammadi@shirazu.ac.ir (H. Mohammadi)

http://dx.doi.org/10.22064/tava.2018.81469.1099

frequently used is micro-sensor in which the information is gathered from the environment by measuring thermal, mechanical or magnetic phenomena. The electronic part then processes this information and responds by moving, positioning, filtering or performing some other mechanical action. Modeling and simulating micro-beams can be a challenging task, since they are scale free and the small-scale effect in their mechanical properties cannot be captured by classical beam theories. For example, it was shown by Wang and Hu [4] that classical beam theories are incapable of predicting the changes in phase velocities of wave propagation in a carbon nanotube with large wavenumber. In order to solve these inconsistencies, many theories of non-classical higher order continuum have been established to consider the size effect. In such theories, some higher-order stresses are usually taken into account besides the classical stress. Furthermore, in higher order theories, there exist material length-scale parameters in addition to the classical material constants in classical continuum theories.

One such higher order theory that takes the size effect into account is the couple-stress theory presented by Koiter [5] and Mindlin and Tiersten [6]. There are two additional higher-order material parameters besides the classical Lame constants in the constitutive equations of this theory. The free vibration behaviour of cellular solids was studied by Su and Liu [7] using the couple-stress theory. The modified couple stress theory was suggested in 2002 by Yang et al. [8]. This theory which has only one higher-order material constant was used by Asghari et al. [9] to obtain a nonlinear Timoshenko beam formulation.

Another popular higher-order theory that considers small-scale effects is the modified strain gradient theory which was presented by Lam et al. [10]. Many researchers have used this theory to study various aspects of micro/nano structures behavior. For example, based on the strain gradient theory, Kahrobaiyan et al. [11] developed a nonlinear size-dependent Euler Bernoulli beam model. In another article, the size-dependent nonlinear forced vibration of an Euler-Bernoulli micro-beam based on the modified strain gradient theory was investigated by Vatankhah et al. [12].

The resolution of micro-sensors is measured by their minimum detectable frequency shifts which are limited by the onset of multivaluedness of the frequency responses. These frequency shifts which are also known as jumps, occur at bifurcation points. It was Poincare who first introduced the concept of bifurcation to show how some system features such as the number of the solutions and their type change qualitatively when one or more system parameter change[13]. Lin and Zhao [14] investigated the bifurcation behavior of a one degree of freedom NEMS electrostatic torsional varactor. In another article, Mobki et al. [15] analyzed the dynamical and bifurcation behavior of a capacitive micro-beam suspended between two fixed electrically conductive plates and subjected to electrostatic forces. Kacem et al. [16] tested a four-bifurcation-point micromechanical resonator which was actuated electrostatically.

In the present paper, the governing equation for the vibration of a damped clamped-clamped micro-beam is derived by taking the Poisson’s effect into consideration and the frequency-response equation is obtained. Then by using a mathematical approach, the bifurcation points of the system are determined and corresponding values of jump-heights are calculated for different values of excitation amplitude and pre-stress load. Also, the effect of length-scale parameters on the bifurcation characteristics of the vibrating micro/nano beam is illustrated.

2. The governing equations

The stress-strain relation in the classical linear theory of elasticity is given by

$$\sigma_{ij} = \lambda\varepsilon_{ij}\delta_{ij} + 2\mu\varepsilon_{ij}. \tag{1}$$

where λ and μ are Lame's coefficients and stress and elastic strain tensors are denoted by σ and ε , respectively.

Assuming a linear elastic material with infinitesimal deformations, the stored strain energy u_m for a continuum that occupies region ϕ based on the modified strain gradient theory is expressed as [10]:

$$u_m = \frac{1}{2}\int_{\phi}\left(\sigma_{ij}\varepsilon_{ij} + p_i\gamma_i + \tau_{ijk}^{(1)}\eta_{ijk}^{(1)} + m_{ij}^{s}\chi_{ij}^{s}\right)dv, \tag{2}$$

where

$$\gamma_i = \varepsilon_{mm,i}, \tag{3}$$

$$\eta_{ijk}^{(1)} = \frac{1}{3}\left(\varepsilon_{jk,i} + \varepsilon_{ki,j} + \varepsilon_{ij,k}\right) - \frac{1}{15}\delta_{ij}\left(\varepsilon_{mm,k} + 2\varepsilon_{mk,m}\right) - \frac{1}{15}\left[\delta_{jk}\left(\varepsilon_{mm,k} + 2\varepsilon_{mi,m}\right) + \delta_{ki}\left(\varepsilon_{mm,j} + 2\varepsilon_{mj,m}\right)\right. \tag{4}$$

$$\chi_{ij}^{s} = \frac{1}{2}\left(\theta_{i,j} + \theta_{j,i}\right), \tag{5}$$

$$\theta_i = \frac{1}{2}\left(\mathrm{curl}\left(\mathbf{u}\right)\right)_i, \tag{6}$$

ui, γ_i and θi represent the components of the displacement vector $\mathbf{u}$, the dilatation gradient vector $\boldsymbol{\gamma}$, and infinitesimal rotation vector $\boldsymbol{\theta}$, respectively and χ_{ij}^{s} is the symmetric part of the curvature tensor.

Considering a linear isotropic elastic material, the relation between components of the stress and the kinematic parameters is described by

$$p_i = 2\mu l_0^2\gamma_i, \tag{7}$$

$$\tau_{ijk}^{(1)} = 2\mu l_1^2\eta_{ijk}^{(1)}, \tag{8}$$

$$m_{ij}^{s} = 2\mu l_2^2\chi_{ij}^{s}, \tag{9}$$

in which p_i and $\tau_{ijk}^{(1)}$ are the work-conjugates to $\varepsilon_{mm,i}$ and $\eta_{ijk}^{(1)}$ respectively, m_{ij}^{s} is the symmetric part of the couple-stress tensor and l_0, l_1 and l_2 are material length scale parameters related to dilatation gradients, deviatoric stretch gradients and rotation gradients, respectively [10].

Schematics for a clamped-clamped Euler Bernoulli beam with preload and transverse distributed load is shown in Fig 1.

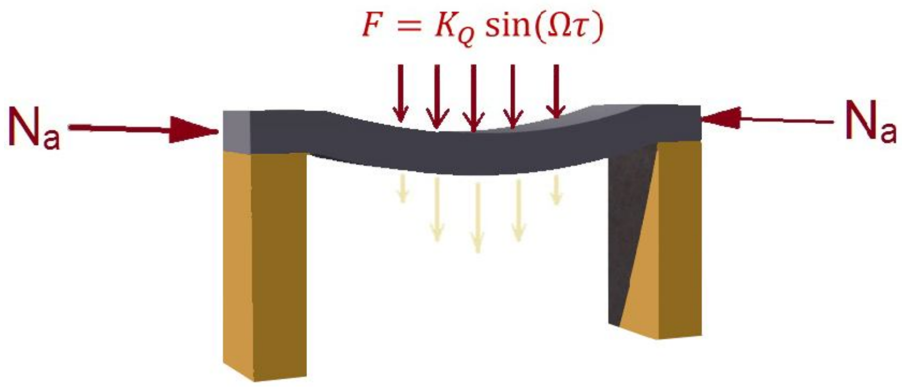

Fig 1. Schematics of a preloaded clamped-clamped micro-beam with distributed transverse loading.

According to the Euler-Bernoulli beam theory, the displacement field can be described as:

$$u_1 = u(x,t) - z\frac{\partial w(x,t)}{\partial x}, \tag{10}$$

$$u_2 = 0, \tag{11}$$

$$u_3 = w(x,t). \tag{12}$$

in which u and w are the axial and vertical displacements, respectively.

Based on von Kármán assumption, the nonlinear strain component can be written as

$$\varepsilon_{11} = \frac{\partial u}{\partial x} - z\frac{\partial^2 w}{\partial x^2} + \frac{1}{2}\left(\frac{\partial w}{\partial x}\right)^2. \tag{13}$$

Now assuming that the stress is uniaxial, one can write:

$$\varepsilon_{22} = \varepsilon_{33} = -v\varepsilon_{11}, \tag{14}$$

where v is the Poisson's ratio. Many other works, e.g. [17, 18] neglect the Poisson's effect. But it is included as an ad-hoc assumption in this research [19].

Using Eqs. (3) to (6), the non-zero components of kinematic parameters and higher order stresses are:

$$\gamma_1 = (1-2v)\left(\frac{\partial^2 u}{\partial x^2} - z\frac{\partial^3 w}{\partial x^3} + \frac{\partial w}{\partial x}\frac{\partial^2 w}{\partial x^2}\right),\ \gamma_3 = -(1-2v)\frac{\partial^2 w}{\partial x^2}, \tag{15}$$

$$\chi_{12}^s = \chi_{21}^s = -\frac{1}{2}\frac{\partial^2 w}{\partial x^2}, \tag{16}$$

$$\eta_{111}^{(1)} = \frac{2}{5}(1+v)\left(\frac{\partial^2 u}{\partial x^2} - z\frac{\partial^3 w}{\partial x^3} + \frac{\partial w}{\partial x}\frac{\partial^2 w}{\partial x^2}\right),\ \eta_{113}^{(1)} = \eta_{311}^{(1)} = \eta_{131}^{(1)} = -\frac{4}{15}(1+v)\frac{\partial^2 w}{\partial x^2}, \tag{17}$$

$$\eta_{122}^{(1)} = \eta_{133}^{(1)} = \eta_{212}^{(1)} = \eta_{221}^{(1)} = \eta_{313}^{(1)} = \eta_{331}^{(1)} = \frac{-1}{5}(1+v)\left(\frac{\partial^2 u}{\partial x^2} - z\frac{\partial^3 w}{\partial x^3} + \frac{\partial w}{\partial x}\frac{\partial^2 w}{\partial x^2}\right), \tag{18}$$

$$\eta_{223}^{(1)}=\eta_{232}^{(1)}=\eta_{322}^{(1)}=\frac{1}{15}(1+v)\frac{\partial^2 w}{\partial x^2},\eta_{333}^{(1)}=\frac{1}{5}(1+v)\frac{\partial^2 w}{\partial x^2}. \tag{19}$$

$$\sigma_{11}=Ee_{11}=E\left(\frac{\partial u}{\partial x}-z\frac{\partial^2 w}{\partial x^2}+\frac{1}{2}\left(\frac{\partial w}{\partial x}\right)^2\right), \tag{20}$$

$$p_1=2\mu l_0^2(1-2v)\left(\frac{\partial^2 u}{\partial x^2}-z\frac{\partial^3 w}{\partial x^3}+\frac{\partial w}{\partial x}\frac{\partial^2 w}{\partial x^2}\right),\ p_3=-2\mu l_0^2(1-2v)\frac{\partial^2 w}{\partial x^2}, \tag{21}$$

$$m_{12}^s=m_{21}^s=-\mu l_2^2\frac{\partial^2 w}{\partial x^2}, \tag{22}$$

$$\tau_{111}^{(1)}=\mu l_1^2\frac{4}{5}(1+v)\left(\frac{\partial^2 u}{\partial x^2}-z\frac{\partial^3 w}{\partial x^3}+\frac{\partial w}{\partial x}\frac{\partial^2 w}{\partial x^2}\right),\ \tau_{113}^{(1)}=\tau_{311}^{(1)}=\tau_{131}^{(1)}=-\mu l_1^2\frac{8}{15}(1+v)\frac{\partial^2 w}{\partial x^2}, \tag{23}$$

$$\tau_{122}^{(1)}=\tau_{133}^{(1)}=\tau_{212}^{(1)}=\tau_{221}^{(1)}=\tau_{313}^{(1)}=\tau_{331}^{(1)}=\frac{-2}{5}\mu l_1^2(1+v)\left(\frac{\partial^2 u}{\partial x^2}-z\frac{\partial^3 w}{\partial x^3}+\frac{\partial w}{\partial x}\frac{\partial^2 w}{\partial x^2}\right), \tag{24}$$

$$\tau_{122}^{(1)}=\tau_{122}^{(1)}=\tau_{122}^{(1)}=\frac{2}{15}\mu l_1^2(1+v)\frac{\partial^2 w}{\partial x^2},\tau_{333}^{(1)}=\frac{2}{5}\mu l_1^2(1+v)\frac{\partial^2 w}{\partial x^2}. \tag{25}$$

Applying initial axial compressive preload $\mathcal{N}_a$ on the beam with constant cross section area *A*, length *L*, moment inertia *I* and Young modulus *E*, taking the effect of $\mathcal{N}_a$ into consideration, one may write the total strain energy based on Eq. (2) as [20]:

$$\begin{aligned}\mathcal{U}=&\frac{1}{2}\int_0^L\int_A(E\left(\frac{\partial u}{\partial x}-z\frac{\partial^2 w}{\partial x^2}+\frac{1}{2}\left(\frac{\partial w}{\partial x}\right)^2\right)^2+\mu\left(2l_0^2(1-2v)^2+l_2^2+\frac{120}{225}l_1^2(1+v)^2\right)\left(\frac{\partial^2 w}{\partial x^2}\right)^2\\&+\mu\left(2l_0^2(1-2v)^2+\frac{4}{5}l_1^2(1+v)^2\right)\left(\frac{\partial^2 u}{\partial x^2}-z\frac{\partial^3 w}{\partial x^3}+\frac{\partial w}{\partial x}\frac{\partial^2 w}{\partial x^2}\right)^2-\frac{2\mathcal{N}_a}{A}\left(\frac{\partial u}{\partial x}-z\frac{\partial^2 w}{\partial x^2}+\frac{1}{2}\left(\frac{\partial w}{\partial x}\right)^2\right))dAdx\\&=\frac{1}{2}\int_0^L(EA\left(\frac{\partial u}{\partial x}+\frac{1}{2}\left(\frac{\partial w}{\partial x}\right)^2\right)^2-2\mathcal{N}_a\left(\frac{\partial u}{\partial x}+\frac{1}{2}\left(\frac{\partial w}{\partial x}\right)^2\right)+k_1\left(\frac{\partial^2 w}{\partial x^2}\right)^2+k_2\left(\frac{\partial^3 w}{\partial x^3}\right)^2\\&+\frac{k_2}{r^2}\left(\frac{\partial^2 u}{\partial x^2}+\frac{\partial w}{\partial x}\frac{\partial^2 w}{\partial x^2}\right)^2)dx,\end{aligned} \tag{26}$$

where

$$k_1=EI+\mu A\left(2l_0^2(1-2v)^2+l_2^2+\frac{120}{225}l_1^2(1+v)^2\right), \tag{27}$$

$$k_2=\mu I\left(2l_0^2(1-2v)^2+\frac{4}{5}l_1^2(1+v)^2\right), \tag{28}$$

$$r=\left(\frac{I}{A}\right)^{0.5}, \tag{29}$$

The virtual work due to other external loads is given by:

$$\delta \mathcal{W} = \int_0^L q\delta w dx, \tag{30}$$

where q is the distributed transverse force.

The kinetic energy of the beam can then be written as

$$T = \frac{1}{2}\int_0^L \rho \int_A \left[\left(\frac{\partial u}{\partial t} - z\frac{\partial^2 w}{\partial x \partial t} \right)^2 + \left(\frac{\partial w}{\partial t} \right)^2 \right] dAdx, \tag{31}$$

in which, ρ is the mass per volume. The total energy can be written in the variational form as

$$\delta T = \int_0^L \rho \int_A \left[\frac{\partial u}{\partial t}\frac{\partial \delta u}{\partial t} - z\frac{\partial u}{\partial t}\frac{\partial^2 \delta w}{\partial x \partial t} - z\frac{\partial^2 w}{\partial x \partial t}\frac{\partial \delta u}{\partial t} + z^2 \frac{\partial^2 w}{\partial x \partial t}\frac{\partial^2 \delta w}{\partial x \partial t} + \frac{\partial w}{\partial t}\frac{\partial \delta u}{\partial t} \right] dAdx. \tag{32}$$

Applying the Hamilton's principle as below, the governing equation can be formed.

$$\int_{t_1}^{t_2} \left(\delta \mathcal{W} - \delta \mathcal{U} + \delta T \right) dt = 0. \tag{33}$$

Now the non-dimensional parameter $b_0 = \frac{r}{L}$ is introduced where L is the length of the beam and r is defined in Eq. (29). The non-dimensional pre-stress load and transverse distributed load are also defined as $N_a = \frac{\mathcal{N}_a L^2}{EI}$ and $Q = \frac{qL^4}{EIr}$ respectively. The rest of the non-dimensional parameters are expressed as:

$$W = \frac{w}{L}, U = \frac{u}{L}, X = \frac{x}{L}, K_1 = \frac{k_1}{EI}, K_2 = \frac{k_2}{EIL^2}, m' = \frac{m_2}{(m_0)L^2}, \tau = \omega_0 t, \omega_0 = \frac{1}{L^2}\sqrt{\frac{EI}{m_0}} \tag{34}$$

It should be noted that in Eq. (34) the parameters m_0 and m_2 are defined as $m_0 = \rho A$ and $m_2 = \rho I$ respectively.

Applying the clamped-clamped boundary conditions, the non-dimensional form of the governing equations of the nonlinear Euler-Bernoulli beam can be obtained [21]:

$$\begin{aligned} &\frac{\partial^2 W}{\partial \tau^2} + C_d \frac{\partial W}{\partial \tau} - m' \frac{\partial^4 W}{\partial X^2 \partial \tau^2} = -K_1 \frac{\partial^4 W}{\partial X^4} + K_2 \frac{\partial^6 W}{\partial X^6} \\ &+ \frac{\partial}{\partial X}\left\{ \left(\frac{1}{b_0^2}\left(\frac{\partial U}{\partial X} + \frac{1}{2}\left(\frac{\partial W}{\partial X} \right)^2 \right) - \frac{K_2}{b_0^2}\frac{\partial^2}{\partial X^2}\left(\frac{\partial U}{\partial X} + \frac{1}{2}\left(\frac{\partial W}{\partial X} \right)^2 \right) - N_a \right) \frac{\partial (W)}{\partial X} \right\} + Q, \end{aligned} \tag{35}$$

$$\frac{\partial^2 U}{\partial \tau^2} = -\frac{\partial}{\partial X}\left\{ -\frac{1}{b_0^2}\left(\frac{\partial U}{\partial X} + \frac{1}{2}\left(\frac{\partial W}{\partial X} \right)^2 \right) + \frac{K_2}{b_0^2}\frac{\partial^2}{\partial X^2}\left(\frac{\partial U}{\partial X} + \frac{1}{2}\left(\frac{\partial W}{\partial X} \right)^2 \right) + N_a \right\}, \tag{36}$$

It is noted that C_d denotes the coefficient of viscous damping.

For these governing equations, the classical boundary conditions are defined as:

$$W\Big|_{X=0}^{X=1}=0, \tag{37}$$

$$\frac{\partial W}{\partial X}\Bigg|_{X=0}^{X=1}=0, \tag{38}$$

$$U\Big|_{X=0}^{X=1}=0, \tag{39}$$

while the non-classical boundary conditions are expressed as follows:

$$\frac{\partial^3 W}{\partial X^3}\Bigg|_{X=0}^{X=1}=0, \tag{40}$$

$$\frac{K_2}{b_0^2}\frac{\partial}{\partial X}\left(\frac{\partial U}{\partial X}+\frac{1}{2}\left(\frac{\partial W}{\partial X}\right)^2\right)=0. \tag{41}$$

Neglecting Poisson's effect and nonlinear terms, Eqs. (35) to (41) reduce to those presented by Akgöz and Civalek [17].

Now, assuming $\frac{\partial^2 U}{\partial \tau^2}=0$, the fourth order differential equation for the transverse motion of the beam can be formed by combining Eqs. (35) and (36).

$$\frac{\partial^2 W}{\partial \tau^2}-m'\frac{\partial^4 W}{\partial X^2\partial \tau^2}+C_d\frac{\partial W}{\partial \tau}+K_1\frac{\partial^4 W}{\partial X^4}-K_2\frac{\partial^6 W}{\partial X^6}+\tilde{N}\frac{\partial^2 W}{\partial X^2}=Q(X,\tau). \tag{42}$$

Where

$$\tilde{N}=-\frac{1}{b_0^2}\int_0^1\frac{1}{2}W'^2dX+N_a \tag{43}$$

3. Solution procedure

The PDE obtained in Eq. (42) can be converted to a time dependent ODE by taking a proper mode shape which satisfies all the classic boundary conditions [22]. Assuming the resonator is subjected to a harmonic concentrated force $Q(X,\tau)=K_Q\sin(\Omega\tau)$ where K_Q is excitation amplitude, using $W(X,t)=\phi(X)W(\tau)$, one can reach the time-dependent ODE by multiplying Eq. (42) by $\phi(X)$ and integrating the resulting equation from 0 to 1. Doing so, the second-order duffing differential equation is obtained as

$$\ddot{W}+\varepsilon^2\eta\dot{W}+\omega_0^2W+\varepsilon^2\alpha W^3=\varepsilon^2K_Q\sin(\Omega\tau), \tag{44}$$

Definitions of parameters α, μ and ω_0 in terms of parameters b_0, C_d, N_a and the length-scale material parameters has been expressed in Appendix A.

Multiple scales method is then applied; hence the solution is considered to be a function of two independent variables instead of one. The underlying idea of this method is to represent the response as a function of multiple time scales instead of a single variable [23].

Here, we express the solution by the following expansion

$$W(\tau,\varepsilon)=W_0(T_0,T_1,T_2)+\varepsilon W_1(T_0,T_1,T_2)+\varepsilon^2 W_2(T_0,T_1,T_2), \tag{45}$$

where $T_0=t$, $T_1=\varepsilon t$, $T_2=\varepsilon^2 t$ and ε is a small parameter that measures the amplitude of oscillation.

In order to study primary resonances of a vibrating micro/nano-beam, a detuning parameter σ is introduced which describes how close the excitation frequency is to the natural frequency ω_0:

$$\Omega=\omega_0+\varepsilon\sigma, \tag{46}$$

Now, by substituting Eq.(45) in Eq.(44) , one can obtain the following system of linear equations based on different powers of ε

$$O(\varepsilon^0): D_0^2 W_0+\omega_0{}^2 W_0=0, \tag{47}$$

$$O(\varepsilon^1): D_0^2 W_1+\omega_0^2 W_1=-2D_0D_1W_0, \tag{48}$$

$$O(\varepsilon^2): D_0^2 W_2+\omega_0^2 W_2=-2D_0D_1W_1-2D_0D_2W_0-D_1^2W_0-\eta D_0W_0-\alpha W_0^3+K_Q\sin(\Omega\tau). \tag{49}$$

The general solution of W_0 can be written as:

$$W_0=A(T_1)\exp(i\omega_0T_0)+\bar{A}(T_1)\exp(-i\omega_0T_0), \tag{50}$$

where $\bar{A}$ is the complex conjugate of A.

Now, by substituting W_0 from Eq. (50) in Eq (48), it is found that any particular solution of Eq.(48) has a secular term containing the factor $\pm\exp(i\omega_0T_0)$ unless:

$$D_1A=0. \tag{51}$$

Elimination of the secular terms in Eq. (49) gives:

$$i\eta A\omega_0+3\alpha A^2\bar{A}+2i\omega_0A'=0. \tag{52}$$

In order to eliminate the secular terms in Eq. (52) , A is written in polar form as below:

$$A=\frac{1}{2}a exp(i\theta). \tag{53}$$

Substituting Eq. (53) in Eq. (52), separating the real and imaginary parts and defining $\gamma=\sigma T_2-\theta$, the set of autonomous equations is obtained:

$$a' = -\eta a + \frac{1}{2}\frac{K_Q}{\omega_0}\sin\gamma, \tag{54}$$

$$a\gamma' = \sigma a - \frac{3}{8}\frac{\alpha}{\omega_0}a^3 + \frac{1}{2}\frac{K_Q}{\omega_0}\cos\gamma. \tag{55}$$

Now by considering the steady-state condition for the motion ($a' = \gamma' = 0$), the system of equations for the primary resonance vibration takes the form of:

$$\eta a = \frac{1}{2}\frac{K_Q}{\omega_0}\sin\gamma, \tag{56}$$

$$\sigma a - \frac{3}{8}\frac{\alpha}{\omega_0}a^3 = -\frac{1}{2}\frac{K_Q}{\omega_0}\cos\gamma. \tag{57}$$

By squaring and adding Eq. (56) and Eq. (57), the frequency-response equation is obtained as:

$$\left(\eta^2 + \left(\sigma - \frac{3}{8}\frac{\alpha}{\omega_0}a^2\right)^2\right).a^2 = \frac{K_Q{}^2}{4\omega_0{}^2}. \tag{58}$$

Bifurcation points of the nonlinear dynamic system can be determined by investigating the sign of the discriminant of Eq. (58) Hence, forming the discriminant of Eq. (58) and setting it equal to zero, one can find the bifurcation points. The mathematical procedure has been carried out in Appendix B.

Now, by solving Eg. (B.3) numerically, one can obtain the two bifurcation points.

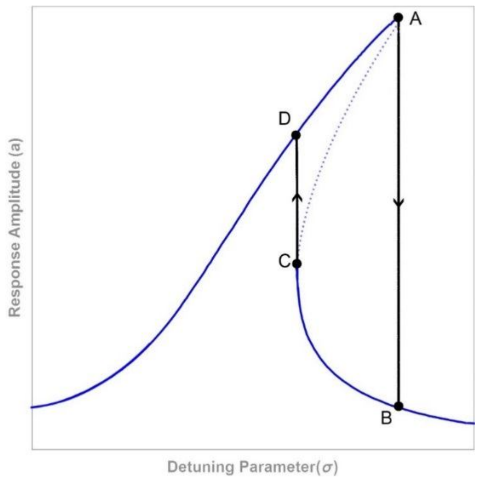

Fig 2. Frequency-response curve for primary resonance Vibration.

Fig 2 depicts the frequency-response curve for a nonlinear system at primary resonance. The two bifurcation points of the system are A and C. As the frequency starts to increase from the beginning, the response amplitude rises slowly until it reaches point A. Point A is the point where the number of solutions changes and the multivaluedness region begins. Now, if the frequency is further increased, a jump-down from point A to point B takes place with a shift in the response amplitude. Now if the analysis is started from the end, by decreasing the frequency, the response amplitude increases slightly until point C is reached. Again, point C is the bifurcation point and therefore there will be a jump up from C to D. The portion of the curve between points A and C is multivaluedness region and cannot be produced experimentally.

4. Results and discussion

It is assumed that the micro-beam is made of Epoxy and its geometrical and material specifications are [24, 25]: E=1.44 GPa, ρ=1200 kg/m^3, μ=521.7 MPa, ν=0.38 and $l_0=l_1=l_2$=17.6 μm. Therefore, the effect of various parameters on the stability and bifurcation behavior of the system can be illustrated numerically.

The effect of preloading stress on the values of bifurcation points is illustrated in Fig 3. It is seen that as the preload increases, the values of the first and second bifurcation points also rise. This indicates that preloading has hardening effect and shifts the multivaluedness range to higher frequencies. Furthermore, it is observed that increasing the excitation amplitude (K_Q) increases the value of the bifurcation points, but doesn't have a significant effect on the slope of the curves.

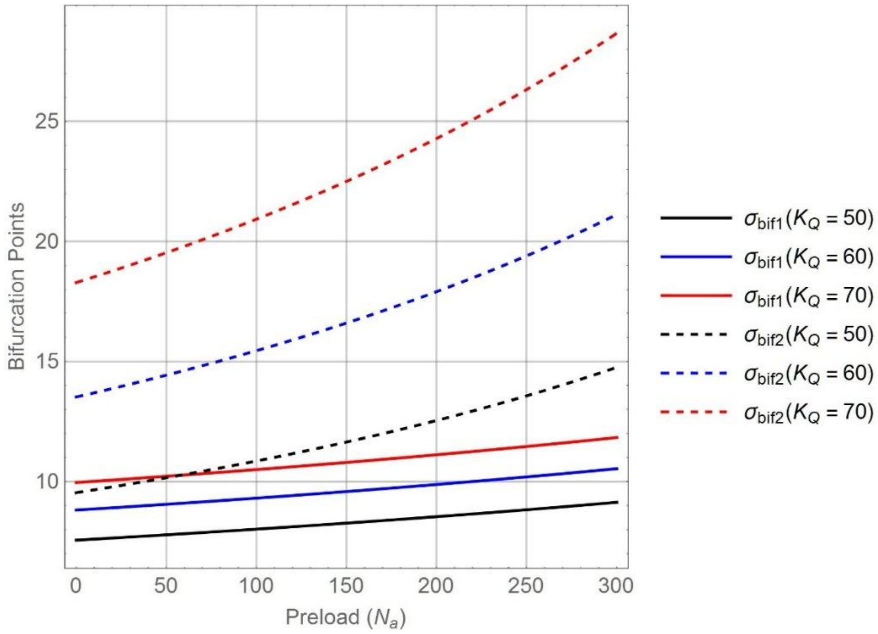

Fig 3. Effects of Preload on the values of the first and second bifurcation points.

Fig 4 illustrates how the range of the multivaluedness region of the micro-resonator changes with the pre-stress load. It is observed that as the axial pre-stress rises, the length of the multivaluedness region of the micro-resonator increases, meaning that for a wider range of frequencies, multivalued response for the dynamical system exists. The same can be said about increasing the excitation amplitude of the system.

The figure shows the length of multivaluedness range for a limited range of preload (N_a) in each ~~cases~~ and they are not plotted for same range of values of preload. It is due to that multivaluedness is obtained for certain values of the parameters. As it is seen that by increasing the excitation amplitude, multivaluedness occurs for smaller range of preload. The same behavior is observed in the following figures.

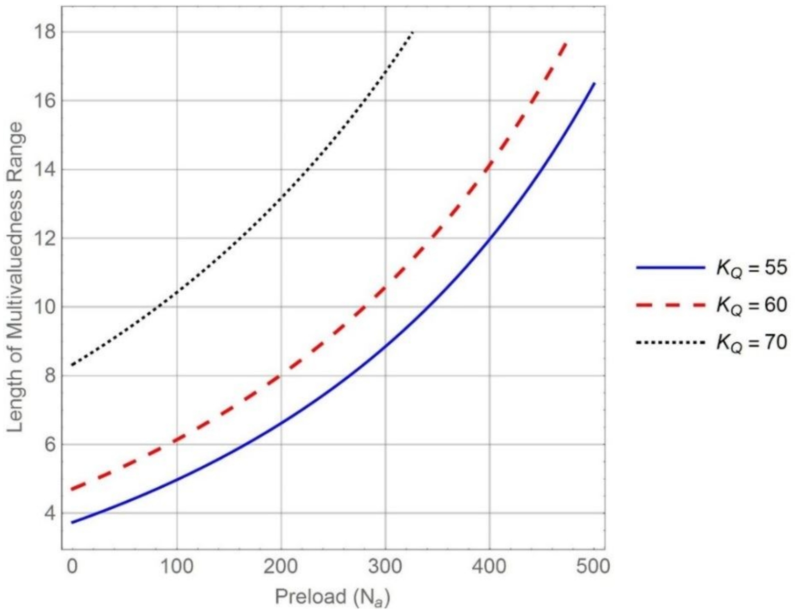

Fig 4. The effects of excitation amplitude (K_Q) on the multivalued region range for the case of primary resonance.

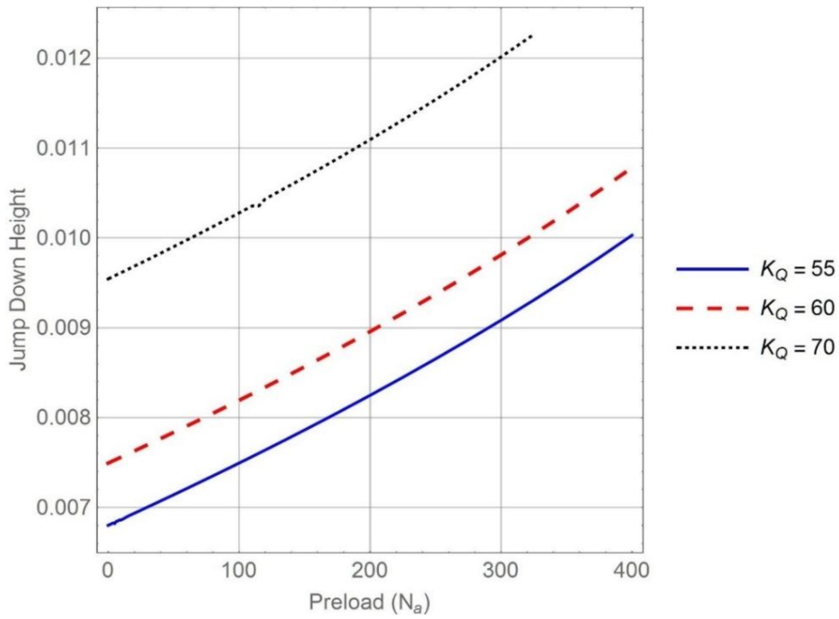

Fig 5. The effects of excitation amplitude (K_Q) on the Jump-down height for the case of primary resonance.

Figure 5 represents the jump-down behavior of the micro-resonator as the pre-stress load is changed. The jump height can be seen as a means to measure the sensitivity of the micro-sensor. It is figured out that as the pre-stress load of the system is increased, the jump-down height increases. The effect of excitation can also be observed on the jump-down height of the micro-sensor. It is understood that higher excitation amplitude leads to a higher jump-height and hence a more sensitive resonator.

Fig 6 illustrates the same effects on the jump-up height of the micro-sensor when point C is reached and the frequency is further decreased. It is seen that the jump-up height rises while the axial preload is being increased. It is also seen that more sensitivity can be achieved by increasing the amplitude of excitation for a primary resonance micro-sensor.

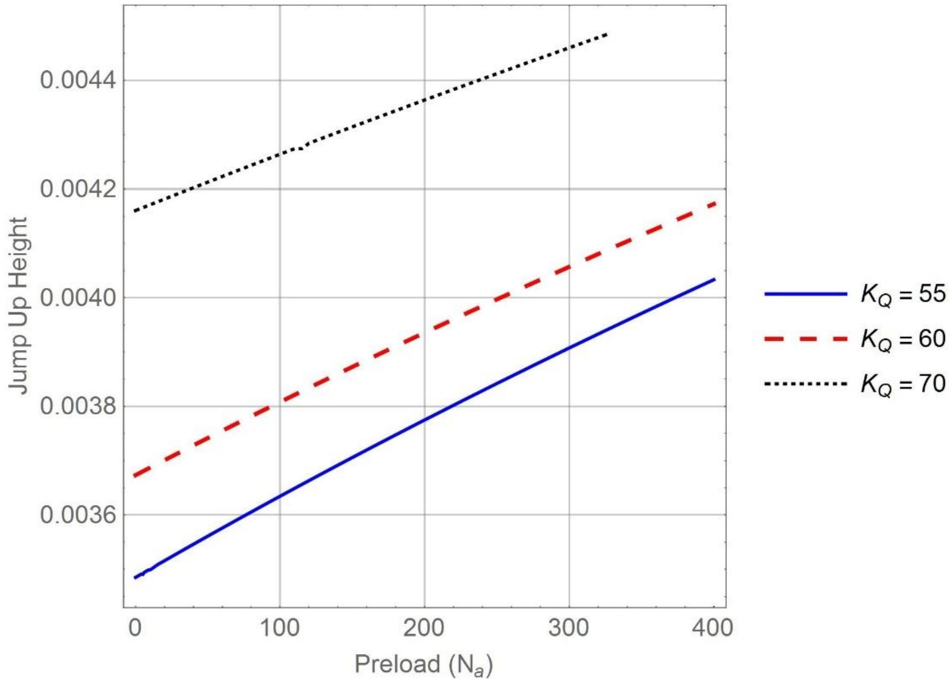

Fig 6. The effects of excitation amplitude (K_Q) on the Jump-up height for the case of primary resonance.

Furthermore, the simultaneous effect of preload and excitation amplitude on the jump-down height at the second bifurcation point is illustrated in Fig 7. By observing Fig 7 it is possible to find the appropriate values for the designing parameter N_a in order to have desired immediate action at the external loading parameters with the certain accuracy.

Also, the effect of the length scale parameters l_0 ,l_1 and l_2 on the length of the multivalued region is illustrated in Fig 8, Fig 9 and Fig 10, respectively. It is seen that increasing the length scale parameters reduces the length of the multivalued region, though not changing the slope. It is also observed that length scale parameters related to the deviatoric stretch gradients (l_1) and rotation gradients (l_2) have more dominant impact on the length of the multivalued region compared to the one corresponding to dilatation gradients (l_0).

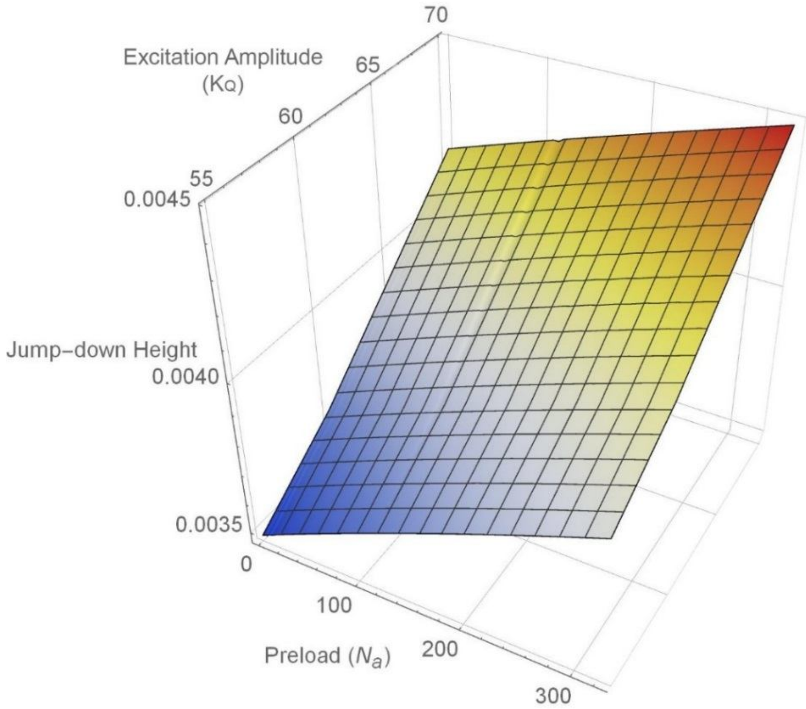

Fig 7. Simultaneous effect of Na and KQ on the jump-down height of primary resonance.

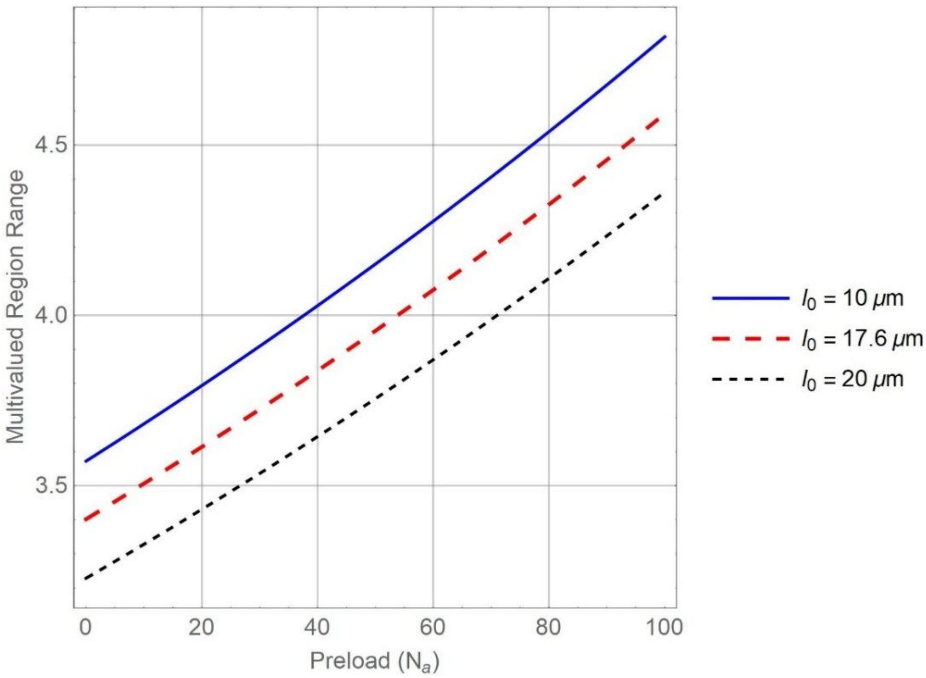

Fig 8. Effect of l_0 on the multivalued region length of primary resonance.

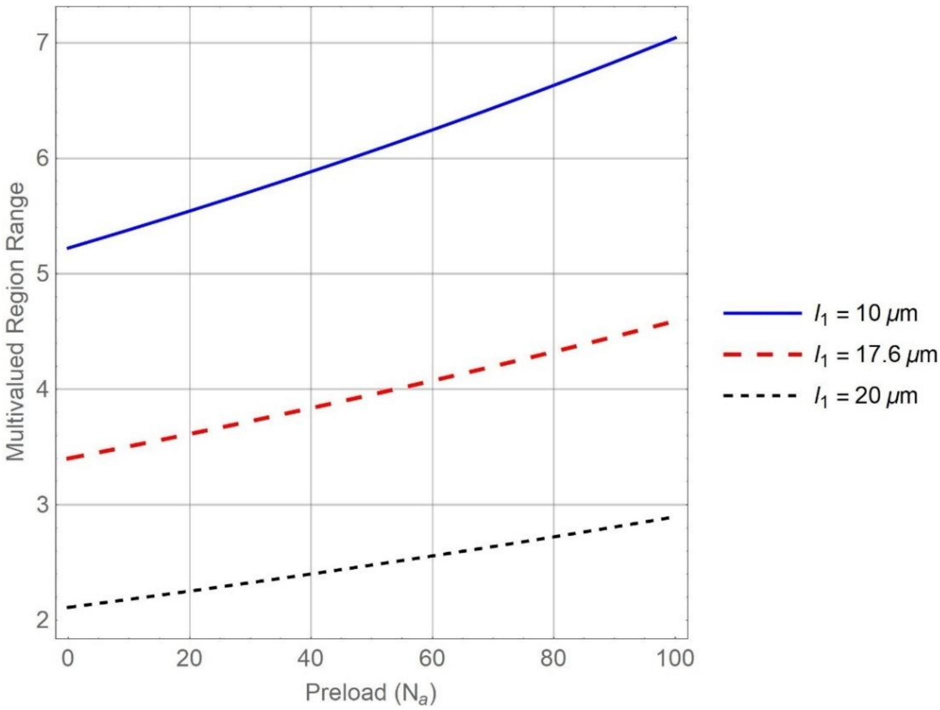

Fig 9. Effect of l1 on the multivalued region length of primary resonance.

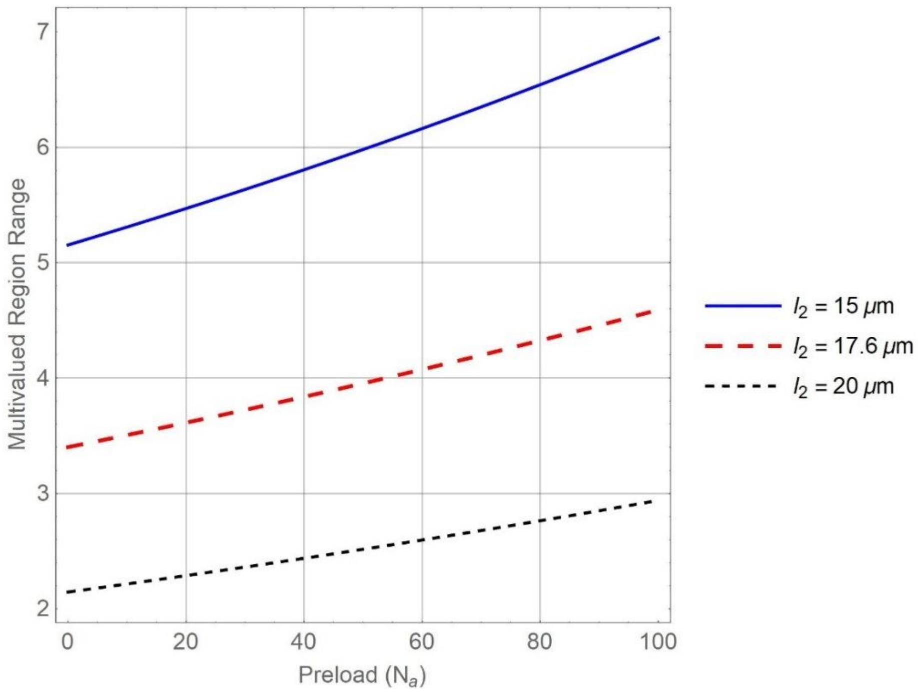

Fig 10. Effect of l_2 on the multivalued region length of primary resonance.

The dimensionless multivaluedness region range and jump heights of a microbeam are listed in Table 1. It is clearly seen that each length-scale parameter has a significant influence on the response of the micro/nano beam. It is also understood from Table 1 that the modified strain gradient theory predicts the range of the multivaluedness region and the jump heights to be smaller in comparison to the modified couple stress and the classical beam theories. The Jump-Down height obtained by the modified strain gradient theory is about half the value obtained by the modified couple stress theory. Hence, it is concluded that the results obtained by the modified couple stress theory and the classical theory are not suitable for micro/nano beams.

Table 1. Dimensionless multivalued region range and jump heights for different higher order beam theories.

Beam Theory	Classical Theory (l_0=l_1=l_2=0)	Modified Couple Stress Theory (l_0=l_1=0 , l_2=17.6)	Modified Strain Gradient Theory (l_0=l_1=l_2=17.6 µm)
Multivaluedness Region Range	58.081	31.941	4.59
Jump-Up Height	0.005291698	0.00430873	0.00355862
Jump-Down Height	0.01759208	0.01362083	0.00721766

The nonlinear response of a clamped-clamped beam which is under a harmonic load of a frequency near the undamped natural frequency is studied by Crespo da Silva [26]. For a numerical comparison, a micro-beam was considered with geometrical and material specifications similar to that of Crespo da Silva. it is seen that the frequency-response curve is in a good agreement with the results obtained by Crespo da Silva [26]. The comparison is depicted in Fig 11.

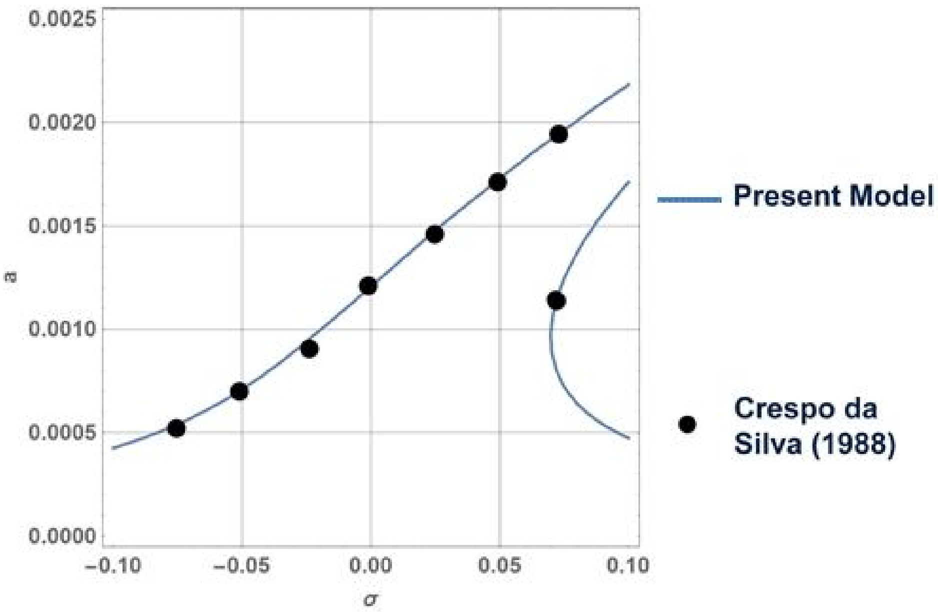

Fig 11. Comparing the results of the presented study with Crespo da Silva's (1998)

5. Conclusion

Unstable dynamical behavior of the mechanical parts of a micro-sensor is one of the major challenges in designing MEMS instruments. Since the nonlinear forced vibration of a micro-beam is size dependent, a nonlinear formulation for the transverse motion of an Euler-Bernoulli micro/nano-beam based on the modified strain Gradient theory is obtained. Multiple Scales Method (MMS) is then applied for solving the nonlinear ODE for W and acquiring the response of the system and a mathematical framework is utilized to find bifurcation points of the dynamic system. Effects of important parameters such as excitation amplitude and pre-stress load on the range of the multivaluedness region and the sensitivity is analyzed. It is observed that as the pre-stress load increases, the range of the multivalued region and the sensitivity also rise. It is further seen that increasing the excitation amplitude (KQ), increases both the multivalued region range and the sensitivity. Also, increasing the length-scale parameters have a softening effect on the response of the system, therefore reduce the range of frequencies for which multiple responses exist. Investigating the effects of such parameters on the dynamic and bifurcation behavior of the micro-sensor enables us to reach an efficient design for desired sensitivity purposes.

Appendix A.

Implementing Galerkin's method with a proper mode shape function which satisfies the boundary conditions, a second order differential equation can be found which is of the following form:

$$\ddot{W}+\varepsilon^2\eta\dot{W}+\omega_0^2W+\varepsilon^2\alpha W^3=\varepsilon^2K_Q\sin\left(\Omega\tau\right), \tag{A.1}$$

which is a cubic duffing equation.
In Eq. (A.1) the coefficients are defined as below:

$$\begin{aligned}\varepsilon^2\eta &= \frac{0.3969C_d}{\left(4.88287m'+0.3669\right)},\\ \omega_0^2 &= \frac{-4.88N_a+198.6K_1+244K_2}{4.8829m'+0.3969},\\ \varepsilon^2\alpha &= \frac{11.92}{b_0^2\left(4.88287m'+0.3669\right)}.\end{aligned} \tag{A.2}$$

Appendix B.

A third order algebraic equation of the form $ax^3+bx^2+cx+d=0$ has a discriminant which can be obtained using the following formula:

$$b^2c^2-4ac^3-4b^3d-27a^2d^2+18abcd \tag{B.1}$$

Now assuming the frequency- response equation can be written as:

$$\left(\eta^2+\left(\sigma-\frac{3}{8}\frac{\alpha}{\omega_0}a^2\right)^2\right).a^2=\frac{K_Q{}^2}{4\omega_0{}^2}. \tag{B.2}$$

the discriminant can be written as:

$$\frac{9}{16}\omega_0^{\,2}\sigma^2\omega_0^{\,2}\left(\frac{\mu^2\omega_0^{\,2}}{4}+\sigma^2\omega_0^{\,2}\right)^2-\frac{9}{16}\omega_0^{\,2}\left(\frac{\mu^2\omega_0^{\,2}}{4}+\sigma^2\omega_0^{\,2}\right)^3-\frac{27\omega_0^{\,3}\sigma^3K_Q}{4096}$$
$$+\frac{243\omega_0^{\,3}\sigma\omega_0\left(\frac{\mu^2\omega_0^{\,2}}{4}+\sigma^2\omega_0^{\,2}\right)K_Q}{32768}-\frac{2187\omega_0^{\,4}K_Q^2}{268435456}=0 \tag{B.3}$$

References

[1] N. Kacem, S. Baguet, S. Hentz, R. Dufour, Computational and quasi-analytical models for non-linear vibrations of resonant MEMS and NEMS sensors, International Journal of Non-Linear Mechanics, 46 (2011) 532-542.
[2] L. Li, Z. Chew, Microactuators: design and technology, in: Smart Sensors and Mems, Elsevier, 2014, pp. 305-348.
[3] Z. Djurić, I. Jokić, A. Peleš, Fluctuations of the number of adsorbed molecules due to adsorption–desorption processes coupled with mass transfer and surface diffusion in bio/chemical MEMS sensors, Microelectronic Engineering, 124 (2014) 81-85.
[4] L. Wang, H. Hu, Flexural wave propagation in single-walled carbon nanotubes, Physical Review B, 71 (2005) 195412.
[5] W. Koiter, Couple-stresses in the theory of elasticity, I and II, Prec, Roy. Netherlands Acad. Sci. B, 67 0964.
[6] R. Mindlin, H. Tiersten, Effects of couple-stresses in linear elasticity, Archive for Rational Mechanics and analysis, 11 (1962) 415-448.
[7] W. Su, S. Liu, Vibration analysis of periodic cellular solids based on an effective couple-stress continuum model, International Journal of Solids and Structures, 51 (2014) 2676-2686.
[8] F. Yang, A. Chong, D.C.C. Lam, P. Tong, Couple stress based strain gradient theory for elasticity, International Journal of Solids and Structures, 39 (2002) 2731-2743.
[9] M. Asghari, M. Kahrobaiyan, M. Ahmadian, A nonlinear Timoshenko beam formulation based on the modified couple stress theory, International Journal of Engineering Science, 48 (2010) 1749-1761.
[10] D.C. Lam, F. Yang, A. Chong, J. Wang, P. Tong, Experiments and theory in strain gradient elasticity, Journal of the Mechanics and Physics of Solids, 51 (2003) 1477-1508.
[11] M.H. Kahrobaiyan, M. Asghari, M. Rahaeifard, M.T. Ahmadian, A nonlinear strain gradient beam formulation, International Journal of Engineering Science, 49 (2011) 1256-1267.
[12] R. Vatankhah, M.H. Kahrobaiyan, A. Alasty, M.T. Ahmadian, Nonlinear forced vibration of strain gradient microbeams, Applied Mathematical Modelling, 37 (2013) 8363-8382.
[13] A.H. Nayfeh, B. Balachandran, Applied nonlinear dynamics: analytical, computational and experimental methods, John Wiley & Sons, 2008.
[14] W.-H. Lin, Y.-P. Zhao, Stability and bifurcation behaviour of electrostatic torsional NEMS varactor influenced by dispersion forces, Journal of Physics D: Applied Physics, 40 (2007) 1649.
[15] H. Mobki, G. Rezazadeh, M. Sadeghi, F. Vakili-Tahami, M.-M. Seyyed-Fakhrabadi, A comprehensive study of stability in an electro-statically actuated micro-beam, International Journal of Non-Linear Mechanics, 48 (2013) 78-85.
[16] N. Kacem, S. Hentz, Bifurcation topology tuning of a mixed behavior in nonlinear micromechanical resonators, Applied Physics Letters, 95 (2009) 183104.
[17] B. Akgöz, Ö. Civalek, Strain gradient elasticity and modified couple stress models for buckling analysis of axially loaded micro-scaled beams, International Journal of Engineering Science, 49 (2011) 1268-1280.
[18] S. Kong, S. Zhou, Z. Nie, K. Wang, Static and dynamic analysis of micro beams based on strain gradient elasticity theory, International Journal of Engineering Science, 47 (2009) 487-498.
[19] H. Mohammadi, M. Mahzoon, Investigating thermal effects in nonlinear buckling analysis of micro beams using modified strain gradient theory, Iranian Journal of Science and Technology. Transactions of Mechanical Engineering, 38 (2014) 303.
[20] H. Mohammadi, M. Mahzoon, Thermal effects on postbuckling of nonlinear microbeams based on the modified strain gradient theory, Composite Structures, 106 (2013) 764-776.

[21] M. Mohammadi, M. Eghtesad, H. Mohammadi, D. Necsulescu, Nonlinear Robust Adaptive Multi-Modal Vibration Control of Bi-Electrode Micro-Switch with Constraints on the Input, Micromachines, 8 (2017) 263.
[22] S.S. Rao, Vibration of continuous systems, John Wiley & Sons, 2007.
[23] A.H. Nayfeh, D.T. Mook, Nonlinear oscillations, John Wiley \& Sons, 2008.
[24] H. Ma, X.-L. Gao, J. Reddy, A microstructure-dependent Timoshenko beam model based on a modified couple stress theory, Journal of the Mechanics and Physics of Solids, 56 (2008) 3379-3391.
[25] S. Park, X. Gao, Bernoulli–Euler beam model based on a modified couple stress theory, Journal of Micromechanics and Microengineering, 16 (2006) 2355.
[26] M.C. Da Silva, Non-linear flexural-flexural-torsional-extensional dynamics of beams—II. Response analysis, International Journal of Solids and Structures, 24 (1988) 1235-1242.